Chemistry Europe
European Chemical Societies Publishing

Special Collection

Singlet Fission in Dideuterated Tetracene and Pentacene

Clemens Zeiser+,[a] Luca Moretti+,[b] Florian Reicherter,[c] Holger F. Bettinger,[c] Margherita Maiuri,[b] Giulio Cerullo,*[b] and Katharina Broch*[a]

The impact of molecular vibrations on singlet fission, which is the spontaneous fission of a singlet exciton into two triplet excitons, is studied using ultrafast optical spectroscopy for the prototypical singlet fission chromophores tetracene and pentacene. We modify the frequency of intramolecular vibrations by deuteration, without impacting thin film structure and molecular arrangement, and study the resulting changes in exo- and endothermic singlet fission rates by comparing the deuterated and parent chromophores. We find that changes in the frequency of the C–C deformation modes of $\Delta\omega = 6\ cm^{-1}$ and the occurrence of C–D vibrational modes do not lead to significant modifications in the singlet fission time constants. We conclude that the changes in the frequency of phonon modes induced by deuteration are too small to significantly impact the electron–phonon coupling that drives the singlet fission process.

1. Introduction

Singlet fission (SF), the photophysical process converting a singlet exciton into two triplet excitons on neighboring molecules, holds promise for increasing solar cell efficiencies.[1] In the last decade, several factors influencing SF rates and efficiencies have been isolated, *inter alia* the energetic difference between singlet and triplet states,[2] charge-transfer contributions, electronic coupling[3–7] and entropic contributions.[5,8]

Recently, the role of molecular vibrations in endo- as well as exothermic SF processes has been discussed, either as a mechanism to overcome the energetic barrier for endothermic SF,[5,9–13] for enabling SF via symmetry breaking[4,14–17] or for promoting the mixing between singlet and triplet states in exothermic SF.[7,12,18–20] This concerns intra- as well as intermolecular vibrations. For example, intramolecular vibrational modes between 300 and 1550 cm^{-1} have been found to be important for efficient SF in acenes[9,17,20,22–25] with a high sensitivity of SF rates to the frequency of the considered modes[17,22,25] and were found to induce vibronic coherences on timescales longer than the singlet fission process itself.[19–21,26–28] Intermolecular vibrations have been discussed as an additional contribution to charge transfer mediated SF via non-adiabatic population transfer[11,20,28] and have been demonstrated to significantly affect SF rates and the subsequent triplet-pair separation process.[27,29–36]

Disentangling the contributions of inter- and intramolecular vibrations to SF is experimentally challenging, since a modification of vibrations via functionalization is often accompanied by changes in molecular arrangement. Here, we use broadband ultrafast transient absorption (TA) spectroscopy to characterize the SF process in neat thin films of dideuterated tetracene and dideuterated pentacene, where intramolecular vibrations are modified compared to the parent compounds, while the thin film structure and the molecular arrangement are not altered. This allows us to solely study the impact of intramolecular vibrations on SF.

2. Results and Discussion

2.1. Raman Spectroscopy

As a first step we performed Raman spectroscopy on thin films of tetracene (TET), 5,12-dideuterated tetracene (D_2-TET), pentacene (PEN) and 6,13-dideuterated pentacene (D_2-PEN) to determine the resulting deuterium shifts of the frequencies of the intramolecular vibrations, see Figure 1 and Table 1, and to compare them with the results of density functional theory calculations at the B3LYP/6-311+G** level, see Figure S4 in the Supporting Information and Table 1. As can be clearly seen, the deuteration results in characteristic changes of C–H deformation modes. For TET the main effect of deuteration on the experimentally determined positions of Raman peaks is a shift

[a] C. Zeiser,+ Prof. K. Broch
Institute for Applied Physics
University of Tübingen
Auf der Morgenstelle 10
72076 Tübingen (Germany)
E-mail: katharina-anna.broch@uni-tuebingen.de
[b] Dr. L. Moretti,+ Dr. M. Maiuri, Prof. G. Cerullo
IFN-CNR, Dipartimento di Fisica
Politecnico di Milano
Piazza Leonardo da Vinci 32
20133 Milan (Italy)
E-mail: giulio.cerullo@polimi.it
[c] F. Reicherter, Prof. Dr. H. F. Bettinger
Institute for Organic Chemistry
University of Tübingen
Auf der Morgenstelle 18
72076 Tübingen (Germany)
[+] These authors contributed equally to this work.

Supporting information for this article is available on the WWW under https://doi.org/10.1002/cptc.202000284
An invited contribution to a Special Collection on Singlet Fission

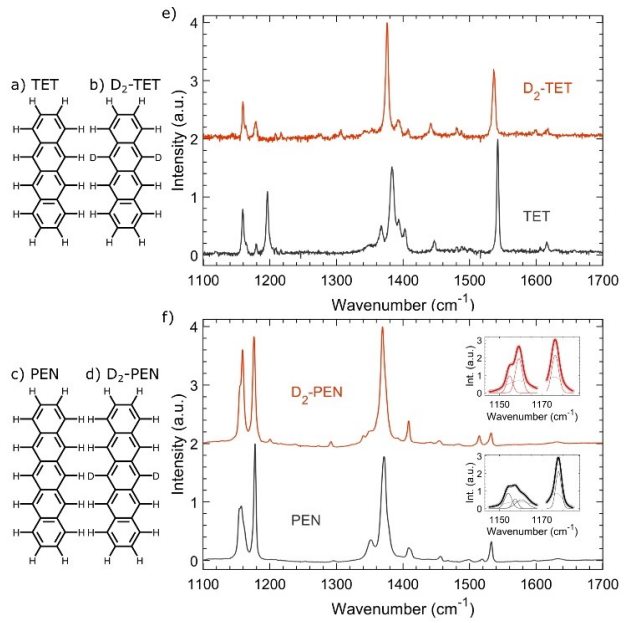

Figure 1. a)–d) Chemical structures of the molecules in this study. e), f) Raman spectra of e) TET and D_2-TET and f) PEN and D_2-PEN with 630 nm excitation. A polynomial background has been subtracted for better comparability.

to lower frequencies of modes by up to $\Delta\omega = 6\ cm^{-1}$ and the disappearance of one C–H deformation mode at $1200\ cm^{-1}$.[37,38] Note that this shift is slightly more pronounced for the calculated modes, see Table 1.

Interestingly, for PEN the deuteration has the most significant impact on the relative intensities of Raman peaks corresponding to intramolecular vibrations with a frequency around $1150\ cm^{-1}$, see inset in Figure 1f. Since the vibration at $1150\ cm^{-1}$ is predicted to strongly affect SF via coupling between S_1 and the vibrationally excited triplet-pair state,[18] changes in this region are expected to impact the SF time constants. For PEN, three main vibrational peaks are found at $1154\ cm^{-1}$, $1157\ cm^{-1}$ and $1160\ cm^{-1}$, see Table 1, which are reduced to two peaks at $1155\ cm^{-1}$ and $1159\ cm^{-1}$ for D_2-PEN. The shift in frequency can be attributed to the replacement of one hydrogen atom by deuterium, also resulting in the change in relative intensities and the FWHM of the peaks compared to PEN. In other frequency ranges, we observe the disappearance of modes characteristic of C–H deformation vibrations (see e.g. the mode at $1352\ cm^{-1}$) and the appearance of modes impacted by the deuterium substitution (see e.g. the modes at $1200\ cm^{-1}$ and $1515\ cm^{-1}$). In contrast to TET, the shift in frequencies is less pronounced in PEN. This is consistent with the calculated normal coordinates and corresponding displacement vectors of the Raman active modes in PEN, see Figure S4 in the Supporting Information.

2.2. X-Ray Diffraction

To exclude any effects of structural changes on SF time constants, we investigated the impact of deuteration on the structural and optical properties of the films. Figure 2 shows reciprocal space maps of thin films of the parent (a,c) and the dideuterated compounds (b,d). From the position of the Bragg-peaks as well as their intensity distribution, it is apparent that the film structure and the structural order are not affected by the deuteration. Both, TET (D_2-TET) and PEN (D_2-PEN) show Bragg-reflexes which indicate a herringbone arrangement of the molecules in the unit cells and which are consistent with literature reports of the parent molecules,[39–42] see Supporting Information for details.

X-ray reflectivity (XRR) scans are shown in Figure 2 e) and f). Consistent with literature, TET and D_2-TET show two series of Bragg-peaks at $q_{z1,TF} = 0.4862\ Å^{-1}$ and $q_{z2,TF} = 0.9706\ Å^{-1}$ and at $q_{z1,B} = 0.5174\ Å^{-1}$ and $q_{z2,B} = 1.033\ Å^{-1}$, which are assigned to the thin-film (TF) and bulk phase (B) of TET films[39] and correspond to an out-of-plane lattice spacing of $d_{TF} = 12.95$ Å and $d_B = 12.16$ Å. In contrast, the XRR-scans of PEN and D_2-PEN show only one prominent series of Bragg-reflexes, consistent with the PEN thin-film phase, at $q_{z1,TF} = 0.4067\ Å^{-1}$ and $q_{z2,TF} = 0.8137\ Å^{-1}$ corresponding to an out-of-plane lattice spacing of $d_{TF} = 15.44$ Å[41,42] and a weaker contribution of the PEN bulk phase at $q_{z2,B} = 0.8704\ Å^{-1}$ ($d_B = 14.44$ Å).[40] Importantly, for both, TET and PEN, we find no indication for differences in the structural order, the out-of-plane lattice spacing or the crystallite size for the dideuterated compound compared to the parent compound.

Table 1. Frequencies ω [cm^{-1}] of the main intramolecular vibrations observed in Figure 1 and comparison with DFT calculations. n.o. indicates modes which are not observed.

TET (exp.)	TET (calc.)	D_2-TET (exp.)	D_2-TET (calc.)	PEN (exp.)	PEN (calc.)	D_2-PEN (exp.)	D_2-PEN (calc.)
			ω [cm^{-1}]				
1159	1151	1160	1157	1154		1155	
1180	1186	1179	1176	1157	1158	1159	1162
1197	1207	n. o.		1160			
1367	1359	n. o.		1178	1185	1176	1185
1383		1376	1347	n. o.		1200	1211
1447	1432	1441	1421	1352	1337	n. o.	
1542	1562	1536	1549	1371		1369	1333
				1409	1420	1408	1418
				n. o.		1515	1497
				1533	1563	1532	1559

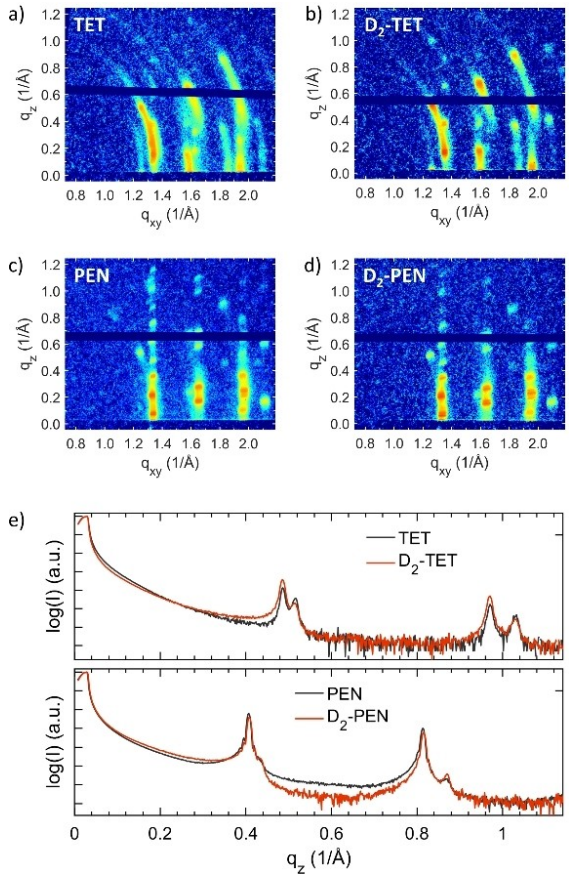

Figure 2. a)–d) Reciprocal space maps and e) X-ray reflectivity scans of thin films of a) TET, b) D_2-TET, c) PEN and d) D_2-PEN.

2.3. Absorption Spectroscopy

Lastly, the absorption spectra of the thin films are shown in Figure 3. For TET and D_2-TET (PEN and D_2-PEN) we observe the main transitions at $\lambda_{1,TET}=519$ nm ($\lambda_{1,PEN}=667$ nm), $\lambda_{2,TET}=506$ nm ($\lambda_{2,PPEN}=629$ nm), $\lambda_{3,TET}=471$ nm ($\lambda_{3,PEN}=582$ nm) and $\lambda_{4,TET}=443$ nm ($\lambda_{4,PEN}=539$ nm), respectively. In all spectra, λ_1 and λ_2 are the Davydov components of the S_0–S_1 transition, split due to the coupling of translationally inequivalent transition dipole moments[43–46] and λ_3 and λ_4 correspond to the excitation of higher vibronic sublevels of the first electronically excited state. For the parent and the deuterated compounds, we find a similar absolute value of the Davydov-splitting of 110 meV for PEN and D_2-PEN and 90 meV for TET and D_2-TET, respectively. The unchanged relative intensities of the Davydov-components of the parent and the deuterated compounds support our conclusion that the molecular arrangement and the intermolecular interactions are not altered by the deuteration.

2.4. Ultrafast Transient Absorption Spectroscopy

Finally, we turn to the investigation of the photophysics and the impact of the modified intramolecular frequencies on the

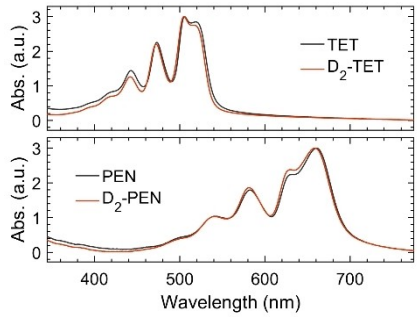

Figure 3. UV-Vis absorption spectra of thin films of TET (upper panel, black), D_2-TET (upper panel, red), PEN (lower panel, black) and D_2-PEN (lower panel, red).

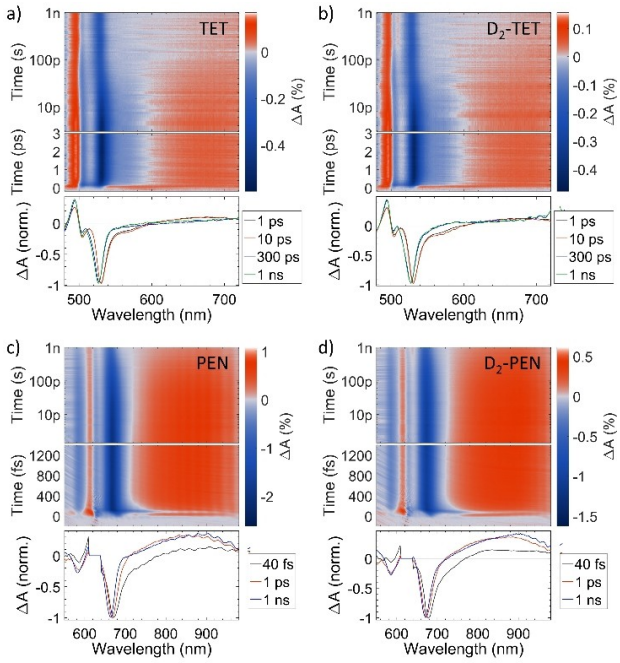

Figure 4. TA maps and normalized TA spectra extracted at different times for the different compounds. a, b) TET and D_2-TET with $\lambda_{exc}=520$ nm and an excitation fluence of 37 μJ/cm^2. c,d) PEN and D_2-PEN with $\lambda_{exc}=620$ nm and a fluence of 31 μJ/cm^2.

SF rates, which we probed using ultrafast TA spectroscopy[47,48] with an excitation wavelength of $\lambda_{exc}=620$ nm and $\lambda_{exc}=520$ nm, for PEN (D_2-PEN) and TET (D_2-TET), respectively, see Figure 4 and 5. The data were analysed using global analysis (GA).[49,50]

In TET, fingerprints for SF are the decrease in the stimulated emission (SE) at 540 nm, the decay of singlet excited-state absorption (ESA) at 680 nm as well as the rise of triplet ESA at longer wavelengths (>700 nm).[51] Signatures at similar positions were also observed for D_2-TET. Indeed, comparing the time traces (Figure 5) extracted at these wavelengths and the position of the ground state bleach (GSB) peaking at 530 nm, we find them to be nearly identical. We note that the signal was strongly affected by singlet-singlet annihilation, leading to a non-exponential decay at early times (see the Supporting

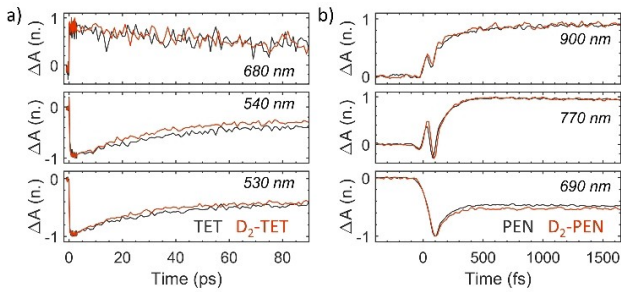

Figure 5. Comparison of time traces extracted from TA measurements at different wavelengths for different compounds. a) TET and D_2-TET with λ_{exc} = 520 nm and 37 μJ/cm². b) PEN and D_2-PEN with λ_{exc} = 620 nm and 31 μJ/cm².

Information for the results of the GA). This non-exponential decay can reasonably well be approximated using two exponential functions as confirmed by the fact that the analysis of TA data taken using three different fluences yields quantitatively similar SF time constants.

For PEN the SF fingerprints are the rise in the triplet ESA at 900 nm and the concomitant decrease in the singlet SE at 690 nm and the GSB at 670 nm.[48] Again, we find both signatures in the D_2-PEN, where they follow a similar time dependence (Figure 5).

In the literature, intra- and intermolecular vibrational modes have been discussed to impact SF in various ways.[4,5,7,9–20] For TET and PEN, several modes have been identified as key contributions, such as the modes at 1440 cm^{-1} and 1540 cm^{-1} in TET[9] or the mode at 1150 cm^{-1}, which is discussed to promote mixing between the singlet and the triplet pair state in PEN.[18,25] Furthermore, while SF in PEN has experimentally been found to be robust against variations in structural properties and intermolecular interaction strength,[52] SF of TET shows a sensitivity to the molecular arrangement.[53] This underlines the importance of a careful structural characterization of the samples to arrive at unambiguous conclusions on the impact of intramolecular vibrations on SF rates. As can be seen in Figure S1–S3, we were able to successfully impact the above-mentioned relevant modes using deuteration without impacting the structural order or the molecular arrangement.

Figure 6 shows the SF time constants of TET and D_2-TET (Figure 6a) as well as PEN and D_2-PEN (Figure 6b) as obtained by a GA, as a function of excitation fluence. The time constants obtained for the parent compounds are in good agreement with those reported in the literature.[44,49,51] The data show that, within the error bars, SF proceeds with the same time constant for the parent and the deuterated compound and the shift in intramolecular vibrations does not lead to measurable changes. This is a rather surprising result. In Ref. [18], a dramatic decrease of the SF rate in PEN was observed upon change in the frequency of the contributing mode by 250 cm^{-1}. Similarly, for TET calculations[9] have shown that those modes which bring S_1 and ^{1}(TT) in energetic resonance also enable the vibronic coupling. Five relevant modes were identified of which the mode at 1432 cm^{-1} is the dominant one. This mode shifts in our experiments and calculations by 6 cm^{-1} and 11 cm^{-1}, respectively, upon deuteration and, in addition, its symmetry changes together with most of the other vibrational modes.

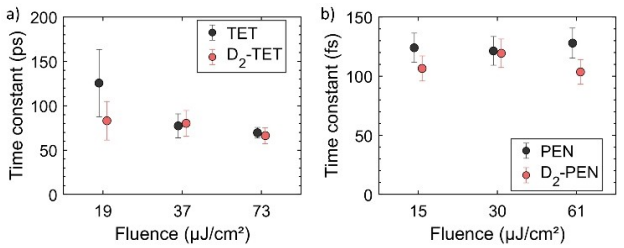

Figure 6. SF time constants obtained from GA of TA measurements on different compounds and at different fluences.

We would like to emphasize that our results do not indicate that current vibronic models are incorrect. They rather show that the changes in the energy of vibrational modes obtained with deuteration are too small to have an effect. Furthermore, calculations[9,18] often focus on few dominant modes, which are identified based on absorption or vibrational spectroscopy. As seen in Figure S4 of our Supporting Information, additional vibrational modes exist in close energetic proximity to these dominant modes. Moving a relevant mode out of energetic resonance might move another mode into energetic resonance, reducing the effect of deuteration. Additional factors such as disorder might also overshadow the effect of deuteration.

3. Conclusion

In conclusion, we used deuteration to modify the frequencies of intramolecular vibrational modes in TET and PEN, which were predicted to mediate SF, without affecting the molecular arrangement or interaction strength. Frequency shifts on the order of 6 cm^{-1}, pronounced changes in relative intensities of vibrational modes and their occurrence did not impact the corresponding SF time constants. From this we conclude that the changes in mode frequencies were too minor to influence the vibronic coupling that drives the SF process.

Experimental Section

Pentacene (PEN, $C_{22}H_{14}$) and tetracene (TET, $C_{18}H_{12}$) were purchased from Sigma-Aldrich and used as received. Dideuterated PEN (6,12-dideuteropentacene, D_2-PEN, $C_{22}H_{12}D_2$) and TET (5,12-dideuterotetracene, D_2-TET, $C_{18}H_{10}D_2$) were synthesized by reduction of the corresponding quinones using sodium borodeuteride (see Supporting Information for NMR spectra and further details).

Thin films of the materials were prepared by organic molecular beam deposition in ultra-high vacuum (base pressure p = 10^{-8} mbar), resulting in a final film thickness of 80 nm determined using a quartz-crystal microbalance and confirmed by X-ray reflectivity measurements. Structural characterization was performed on a 3303TT diffractometer (GE) with 1D detector (Meteor 1D, XRD Eigenmann) for X-ray reflectivity (XRR) and on a Xeuss 2.0 SAXS/WAXS system (Xenocs) with a Dectris Pilatus3R 300 K detector for grazing incidence X-ray wide angle scattering (GIWAXS), in both cases using a wavelength of 1.5406 Å.

Absorption spectra were measured using a Lambda 950 spectrophotometer (Perkin-Elmer). Raman spectroscopy was performed on a Labram HR Raman spectrometer (Horiba Jobin-Yvon) with excitation at $\lambda = 632$ nm.

Ultrafast TA experiments were performed using a Ti:Sapphire chirped pulse amplified source (Coherent Libra), with 4 mJ output energy, 1 kHz repetition rate, 800 nm central wavelength and 100 fs pulse duration. Visible excitation pulses with $\approx$70-fs duration and 620 nm wavelength were generated for PEN and D_2-PEN by an optical parametric amplifier (OPA) pumped by the second harmonic of Ti:sapphire using a β-barium borate crystal. For TET and D_2-TET the second harmonic of Ti:sapphire was directly used for excitation. The white-light continuum (WLC) for the broadband probe pulses was achieved in two ways: For TET and D_2-TET a WLC spanning 450 nm–770 nm was obtained by focusing the 800 nm pulses into a 2-mm-thick sapphire plate, while for PEN and D_2-PEN a WLC spanning 540–1000 nm was obtained by focusing the 1200-nm output of a second OPA into a 3-mm-thick YAG plate. The pump pulses were focused to a 350 μm diameter spot, while the probe pulses were focused to a 175 μm diameter spot. TA spectra were collected by using a fast optical multichannel analyzer working at the full 1-kHz laser repetition rate. The measured quantity is the differential transmission, $\Delta T/T$, from which the differential absorbance is calculated as: $\Delta A \cong -\Delta T/T$. Measurements were performed at room temperature and under vacuum to avoid sample degradation. For the global analysis (GA) of the obtained TA data the open source software Glotaran was used.[50]

Acknowledgements

This project has received funding from the European Union's Horizon 2020 research and innovation programme under grant agreement LASERLAB-Europe n.871124 (CUSBO002670) and the DFG (BR 4869/4-1). The authors acknowledge support by the state of Baden-Württemberg through bwHPC and the German Research Foundation (DFG) through grant no INST 40/575-1 FUGG (JUSTUS 2 cluster). C. Z. and K. B. thank Prof. Schreiber (University of Tübingen) for access to equipment.

Conflict of Interest

The authors declare no conflict of interest.

Keywords: singlet fission · deuteration · acenes · ultrafast spectroscopy · transient absorption spectroscopy

[1] M. Einzinger, T. Wu, J. F. Kompalla, H. L. Smith, C. F. Perkinson, L. Nienhaus, S. Wieghold, D. N. Congreve, A. Kahn, M. G. Bawendi, M. A. Baldo, *Nature* **2019**, *571*, 90–94.
[2] M. B. Smith, J. Michl, *Chem. Rev.* **2010**, *110*, 6891–6936.
[3] S. R. Yost, J. Lee, M. W. B. Wilson, T. Wu, D. P. McMahon, R. R. Parkhurst, N. J. Thompson, D. N. Congreve, A. Rao, K. Johnson, et al., *Nat. Chem.* **2014**, *6*, 492–497.
[4] A. M. Alvertis, S. Lukman, T. J. H. Hele, E. G. Fuemmeler, J. Feng, J. Wu, N. C. Greenham, A. W. Chin, A. J. Musser, *J. Am. Chem. Soc.* **2019**, *141*, 17558–17570.
[5] W.-L. Chan, M. Ligges, A. Jailaubekov, L. Kaake, L. Miaja-Avila, X.-Y. Zhu, *Science* **2011**, *334*, 1541–1545.
[6] E. C. Alguire, J. E. Subotnik, N. H. Damrauer, *J. Phys. Chem. A* **2014**, *119*, 299.
[7] E. G. Fuemmeler, S. N. Sanders, A. B. Pun, E. Kumarasamy, T. Zeng, K. Miyata, M. L. Steigerwald, X.-Y. Zhu, M. Y. Sfeir, L. M. Campos, N. Ananth, *ACS Cent. Sci.* **2016**, *2*, 316.
[8] A. B. Kolomeisky, X. Feng, A. I. Krylov, *J. Phys. Chem. C* **2014**, *118*, 5188–5195.
[9] A. F. Morrison, J. M. Herbert, *J. Phys. Chem. Lett.* **2017**, *8*, 1442.
[10] P. M. Zimmerman, F. Bell, D. Casanova, M. Head-Gordon, *J. Am. Chem. Soc.* **2011**, *133*, 19944.
[11] P. M. Zimmerman, C. B. Musgrave, M. Head-Gordon, *Acc. Chem. Res.* **2013**, *46*, 1339.
[12] G. Tao, *J. Chem. Phys.* **2019**, *151*, 054308.
[13] D. Casanova, *J. Chem. Theory Comput.* **2013**, *10*, 324.
[14] H. Tamura, M. Huix-Rotillant, I. Burghardt, Y. Olivier, D. Beljonne, *Phys. Rev. Lett.* **2015**, *115*, 107401.
[15] M. A. Castellanos, P. Huo, *J. Phys. Chem. Lett.* **2017**, *8*, 2480–2488.
[16] X. Xie, A. Santana-Bonilla, W. Fang, C. Liu, A. Troisi, H. Ma, *J. Chem. Theory Comput.* **2019**, *15*, 3721.
[17] K. Miyata, Y. Kurashige, K. Watanabe, T. Sugimoto, S. Takahashi, S. Tanaka, J. Takeya, T. Yanai, Y. Matsumoto, *Nat. Chem.* **2017**, *9*, 983.
[18] R. Tempelaar, D. R. Reichman, *J. Chem. Phys.* **2018**, *148*, 244701.
[19] A. A. Bakulin, S. E. Morgan, T. B. Kehoe, M. W. B. Wilson, A. W. Chin, D. Zigmantas, D. Egorova, A. Rao, *Nat. Chem.* **2016**, *8*,16.
[20] A. J. Musser, M. Liebel, C. Schnedermann, T. Wende, T. B. Kehoe, A. Rao, P. Kukura, *Nat. Phys.* **2015**, *11*, 352.
[21] Y. Fujihashi, L. Chen, A. Ishizaki, J. Wang, Y. Zhao, *J. Chem. Phys.* **2017**, *146*, 044101.
[22] T. C. Berkelbach, M. S. Hybertsen, D. R. Reichman, *J. Chem. Phys.* **2014**, *141*, 074705.
[23] E. Busby, T. C. Berkelbach, B. Kumar, A. Chernikov, Y. Zhong, H. Hlaing, X.-Y. Zhu, T. F. Heinz, M. S. Hybertsen, M. Y. Sfeir, D. R. Reichman, C. Nuckolls, O. Yaffe, *J. Am. Chem. Soc.* **2014**, *136*, 10654.
[24] G. H. Deng, Q. Wei, J. Han, Y. Qian, J. Luo, A. R. Harutyunyan, G. Chen, H. Bian, H. Chen, Y. Rao, *J. Chem. Phys.* **2019**, *151*, 054703.
[25] J. E. Elenewski, U. S. Cubeta, E. Ko, H. Chen, *J. Phys. Chem. C* **2017**, *121*, 11159.
[26] C. Grieco, E. R. Kennehan, A. Rimshaw, M. M. Payne, J. E. Anthony, J. B. Asbury, *J. Phys. Chem. Lett.* **2017**, *8*, 5700–5706.
[27] H. L. Stern, A. Cheminal, S. R. Yost, K. Broch, S. L. Bayliss, K. Chen, M. Tabachnyk, K. Thorley, N. Greenham, J. M. Hodgkiss, J. Anthony, M. Head-Gordon, A. J. Musser, A. Rao, R. Friend, *Nat. Chem.* **2017**, *9*, 1205.
[28] C. Schnedermann, A. M. Altertis, T. Wende, S. Lukman, J. Feng, F. A. Y. N. Schröder, D. H. B. Turban, J. Wu, N. D. M. Hine, N. C. Greenham, A. W. Chin, A. Rao, P Kukura, A. J. Musser, *Nat. Commun.* **2019**, *10*, 4207.
[29] N. Renaud, F. C. Grozema, *J. Phys. Chem. Lett.* **2015**, *6*, 360.
[30] S. Ito, T. Nagami, M. Nakano, *J. Photochem. Photobiol. C* **2018**, *34*, 85.
[31] K. M. Felter, F. C. Grozema, *J. Phys. Chem. Lett.* **2019**, *10*, 7208.
[32] A. Japahuge, T. Zeng, *ChemPlusChem* **2018**, *83*, 146.
[33] B. Carlotti, I. K. Madu, H. Kim, Z. Cai, H. Jiang, A. K. Muthike, L. Yu, P. M. Zimmeran, T. Goodson III, *Chem. Sci.* **2020**, *11*, 8757.
[34] S. R. Ellis, D. R. Dietze, T. Rangel, F. Brouwn-Altvater, J. B. Neaton, R. A. Mathies, *J. Phys. Chem. A* **2019**, *123*, 3863.
[35] Y. Kobori, M. Fuki, S. Nakamura, T. Hasobe, *J. Phys. Chem. B* **2020**, *124*, 9411.
[36] K. Shizu, C. Adachi, H. Kaji, *J. Phys. Chem. A* **2020**, *124*, 3641.
[37] A. I. Alajtal, H. G. M. Edwards, M. A. Elbagerma, I. J. Scowen, *Spectrochim. Acta Part A* **2010**, *76*, 1–5.
[38] Y. Yamakita, J. Kimura, K. Ohno, *J. Chem. Phys.* **2007**, *126*, 064904.
[39] R. K. Nahm, J. R. Engstrom, *J. Chem. Phys.* **2017**,*146*, 52815.
[40] R. B. Campbell, J. M. Robertson, J. Trotter, *Acta Crystallogr.* **1962**, *15*, 289–290.
[41] C. C. Mattheus, A. B. Dros, J. Baas, G. T. Oostergetel, A. Meetsma, J. L. de Boer, T. T. M. Palstra, *Synth. Met.* **2003**, *138*, 475–481.
[42] S. Schiefer, M. Huth, A. Dobrinevski, B. Nickel, *J. Am. Chem. Soc.* **2007**, *129*, 10316.
[43] J. J. Burdett, D. Gosztola, C. J. Bardeen, *J. Chem. Phys.* **2011**, *135*, 214508.
[44] W. Hofberger, H. Bässler, *Phys. Status Solidi B* **1975**, *69*, 2.
[45] M. Dressel, B. Gompf, D. Faltermeier, A. K. Tripathi, J. Pflaum, M. Schubert, *Opt. Express* **2008**, *16*, 19770–19778.
[46] A. Hinderhofer, U. Heinemeyer, A. Gerlach, S. Kowarik, R. M. J. Jakobs, Y. Sakamoto, T. Suzuki, F. Schreiber, *J. Chem. Phys.* **2007**, *127*, 194705.
[47] R. Berera, G. F. Moore, I. H. M. Van Stokkum, G. Kodis, P. A. Liddell, M. Gervaldo, R. Van Grondelle, J. T. M. Kennis, D. Gust, T. A. Moore, A. L. Moore, *Photochem. Photobiol. Sci.* **2006**, *5*, 1142–1149.

[48] M. W. B. Wilson, A. Rao, J. Clark, R. S. S. Kumar, D. Brida, G. Cerullo, R. H. Friend, *J. Am. Chem. Soc.* **2011**, *133*, 11830–11833.
[49] I. H. M. Van Stokkum, D. S. Larsen, R. Van Grondelle, *Biochim. Biophys. Acta Bioenerg.* **2004**, *1657*, 82–104.
[50] J. J. Snellenburg, S. Laptenok, R. Seger, K. M. Mullen, I. H. M. Van Stokkum, *J. Stat. Softw.* **2012**, *49*, 1–22.
[51] M. W. B. Wilson, A. Rao, K. Johnson, S. Gélinas, R. di Pietro, J. Clark, R. H. Friend, *J. Am. Chem. Soc.* **2013**, *135*, 16680–16688.
[52] K. Broch, J. Dieterle, F. Branchi, N. J. Hestand, Y. Olivier, H. Tamura, C. Cruz, V. M. Nichols, A. Hinderhofer, D. Beljonne, F. C. Spano, G. Cerullo, C. J. Bardeen, F. Schreiber, *Nat. Commun.* **2018**, *9*, 954.
[53] D. H. Arias, J. L. Tyerson, J. D. Cood, N. H. Damrauer, J. C. Johnson, *Chem. Sci.* **2016**, *7*, 1185–1191.

Manuscript received: November 30, 2020
Revised manuscript received: March 29, 2021
Accepted manuscript online: March 29, 2021
Version of record online: ■■, ■■■■

ARTICLES